Growth of Ordered Arrangements of One-Dimensional Germanium Nanostructures with Controllable Crystallinities

Nikolay Petkov,[†,‡] Pavels Birjukovs,[§] Richard Phelan,[†] Michael A. Morris,[†,‡] Donats Erts,[‡,§] and Justin D. Holmes*[,†,‡]

Department of Chemistry, Materials Section and Supercritical Fluid Centre, University College Cork, Cork, Ireland, Centre for Research on Adaptive Nanostructures and Nanodevices (CRANN), Trinity College Dublin, Dublin 2, Ireland, and Institute of Chemical Physics, University of Latvia, LV-1586 Riga, Latvia

Received October 10, 2007. Revised Manuscript Received December 8, 2007

Channelled templates such as anodic alumina membranes (AAMs) can be utilized to host, isolate, and guide the growth of one-dimensional (1D) nanostructures. In this study, we present a method for Au-seeded and confined growth of 1D Ge nanostructures with controlled crystallinities and electrical properties within the channels of AAMs. Our approach combines Au nanoparticle seeded growth of semiconductor nanowires by supercritical fluid−liquid–solid (SFLS) mechanism and the highly anisotropic structure of the aligned channels in AAMs. Au seeds with nanosized dimensions were prepositioned inside channelled substrates, followed by SFLS growth at temperatures slightly higher than the Au/Ge eutectic point. Microscopy and XRD measurements reveal that the 1D nanostructures can be obtained with tuneable and controllable crystallinity, grain size and domain boundaries, ranging from chains of Au-nanoparticles connected through semiconductor Ge nanocrystallities, to Au-seeded Ge single crystalline nanowires. Conditions that control the type of Ge nanostructures are (i) the distribution and size of the Au seeds across the alumina surfaces, (ii) the type of SCF deposition, e.g., batch versus flow-through deposition. Additionally, we present electrical data of the ordered arrays of 1D nanostructures, measured by conductive atomic force microscopy (c-AFM), and contrast the data to that previously obtained for similar systems.

Introduction

Ultimately, the successful incorporation of nanowires into optical and electronic devices will require their assembly into electrically addressable high density architectures so that their unique transport properties, either individually or collectively, can be utilized. A variety of methods have been developed for growing "template-free" single crystalline nanowires. Among them Au-seeded growth by the vapor–liquid–solid (VLS) method has gained much attention.[1] Many research groups have successfully combined the VLS approach with laser ablation techniques to synthesize a variety of different nanowires, including Si, Ge, GaAs, GaP, and InP.[2] An extension of the VLS approach using supercritical fluids, known as supercritical fluid-liquid–solid (SFLS) methods, have recently been developed for producing single crystalline Ge and Si nanowires.[3] These nontemplated nanowires have been isolated and utilized to fabricate various nanowire devices, including field-effect transistors, integrated logic gates, memory devices, nanolasers, photodetectors etc.[1,4] The integration of these nanostructures into nanowire-based devices has been achieved either by post synthesis assembly or by "in-place" Au-seeded growth on different substrates. As a result, first examples of single nanowire transistors such as vertically integrated nanowire field-effect transistors (VINFET) and planar integrated nanowire field-effect transistors (PINFET) have been realized.[4]

Channelled templates such as anodic alumina membranes (AAMs) can be utilized to host, isolate and guide the growth of 1D nanostructures.[5] Techniques such as chemical vapor deposition (CVD), electrochemical deposition, electroless deposition and sol–gel methods have being commonly employed to deposit a wide range of nanostructures, such

* To whom correspondence should be addressed. Tel: 353 (0)21 4903608. Fax 353 (0)21 4274097. E-mail: j.holmes@ucc.ie.
† University College Cork.
‡ Trinity College Dublin.
§ University of Latvia.

(1) (a) For example, see the following reviews and the references therein: Thelander, C.; Agarwal, P.; Brongersma, S.; Eymery, J.; Feiner, L. F.; Forchel, A.; Scheffler, M.; Reiss, W.; Ohlsson, B. J.; Goesele, U.; Samuelson, L. *Mater. Today* **2006**, *9*, 28. (b) Lieber, C. M.; Wang, Z. L. *MRS Bull.* **2007**, *32*, 99. (c) Fan, H. J.; Werner, P.; Zacharias, M. *Small* **2006**, *2*, 700.

(2) (a) Nguyen, P.; Ng, H. T.; Meyyappan, M. *Adv. Mater.* **2005**, *17*, 549. (b) Skoeld, N.; Karlsson, L. S.; Pistol, M-E.; Seifert, W.; Traegardh, J.; Samuelson, L. *Nano Lett.* **2005**, *5*, 1943. (c) Morales, A. M.; Lieber, C. M. *Science* **1998**, *279*, 208. (d) Duan, X.; Lieber, C. M. *Adv. Mater.* **2000**, *12*, 298. (e) Wu, Y.; Fan, R.; Yang, P *Nano Lett.* **2002**, *2*, 83. (f) Dailey, J. W.; Taraci, J.; Clement, T.; Smith, D. J.; Drucker, J.; Picraux, S. T. *J. Appl. Phys.* **2004**, *96*, 7556.

(3) (a) Holmes, J. D.; Johanston, K.; Doty, C.; Korgel, B. A. *Science* **2000**, *287*, 1471. (b) Tuan, H.-Y.; Lee, D. C.; Hanrath, T.; Korgel, B. A. *Chem. Mater.* **2005**, *17*, 5705. (c) Hanrath, T.; Korgel, B. A. *Adv. Mater.* **2005**, *15*, 437.

(4) (a) Hang, Yu.; Duan, X.; Wei, Q.; Lieber, C. M. *Science* **2001**, *291*, 630. (b) Agarwal,; Vijayaraghavan, M. N.; Neuilly, F.; Hijzen, E.; Hurkx, G. A. M.; Huang, Yu.; Duan, X.; Wei, Q. *Nano Lett.* **2007**, *7*, 896. (c) Schmidt, V.; Riel, H.; Senz, S.; Riess, W.; Goesele, U. *Small* **2006**, *2*, 85. (d) Goldberg, J.; Hochbaum, A. I.; Yang, P. *Nano Lett.* **2006**, *6*, 973.

(5) (a) For example, see the following reviews and the references therein Steinhart, M.; Wehrspohn, R. B.; Goesele, U.; Wendorff, J. H. *Angew Chem., Int. Ed* **2004**, *43*, 1334. (b) Zhu, J.; Jun, L. *Nanotechnology* **2006**, *17*, S262. (c) Martin, C. R. *Science* **1994**, *266*, 1961. (d) Mallouk, T. E. *Science* **2001**, *291*, 443.

10.1021/cm702923k CCC: $40.75
Published on Web 01/31/2008

as carbon nanotubes, metals, oxides and semiconducting nanowires, inside the pores of AAMs.[5,6] Complimenting these synthetic methods, our group have pioneered the development of supercritical fluid (SCF) inclusion-phase techniques for preparing semiconductor nanostructures within the pores of the AAMs.[7] These SCF processes involve the decomposition of suitable precursors at high temperatures and pressures which fill the pores of the support. However, considerable effort is required with the SCF methodologies to prevent blocking of the pores and to minimize undesirable surface coatings during the deposition process.

Nevertheless, considerable progress has been made in the integration of 1D nanostructures in functional devices, rapid electrical characterization and reliable electrical transport measurements of individual or groups of nanowires is still challenging. To date, the most commonly used method for electrically characterizing 1D nanostructures involves contacting isolated nanowires with metal contacts in a four probe configuration, whereas little progress has been made on the electrical characterization of ordered arrangements of nanowires. Noticeable examples are the electrical properties of aligned surfactant stabilized nanowires, "in-place" grown Si nanowires and our own investigations on semiconductor nanowires encapsulated in AAMs.[8] Specifically, individually doped and undoped Ge nanowires grown by Au seeds were electrically contacted in a two probe configuration and showed resistivities in the range of 1×10^{-4} to 0.3 ohm m.[9] Previous measurements of the electrical properties of ordered arrays of intrinsic Ge nanowires within AAMs gave very high resistivities that were attributed to possible contact problems, the poorly defined crystallinity of the nanowires and large numbers of surface states.[8d]

To date, there have been no reports on Au-seeded growth of Ge nanostructures within ordered channel substrates using supercritical fluid methodologies. Moreover loading factors, crystallinty and domain boundaries of embedded 1D semiconductor nanostructures grown within channelled substrates have not been investigated in detail. This study addresses these points by presenting a method for the confined growth of one-dimensional Ge nanostructures, of defined crystallinity, within the channels of AAMs. Our approach combines the Au nanoparticle seeded growth of semiconductor nanowires by SFLS with the highly anisotropic structure of the aligned channels in AAMs. Au seeds with nanosized dimensions were prepositioned inside the channel substrates, followed by SFLS growth at temperatures slightly higher than the Au/Ge eutectic point. By controlling the growth conditions during the SFLS deposition process, single crystalline or polycrystalline Ge nanostructures are obtainable. Additionally, we present electrical data on the ordered arrays of 1D nanostructures, measured by conductive atomic force microscopy (c-AFM), and contrast the data to that previously obtained for similar systems.

Experimental Section

Synthesis. The AAMs with mean pore diameters of 70–80 nm were prepared following well-established literature methods and showed well-ordered hexagonal arrangements of vertically aligned channels.[8d] The oxide surface was modified with an organo-silane, resulting in covalently anchored primary amine groups. Briefly, the substrates were immersed in 10 mL of dry toluene containing 700 μL of aminopropyltriethoxy silane (Fluka) under refluxing conditions applying standard Schlenk-line techniques. In the second step, 30 mM $H[AuCl_4]$ solutions were used to impregnate the amino-modified substrates for 12 h, and after washing with copious amounts of water, the samples were left for 6 days in air. During the course of these reactions, Au seeds were introduced within the channeled substrates that were used for the SFLS growth. Two types of SFLS growth was employed: (i) batch reaction, where the substrates were introduced inside a high pressure reactor loaded with 10 mL hexane and containing 100 μL of diphenyl germane (denoted as B-SFLS growth), and (ii) injection flow-through reaction, where the precursor mixture (10 mL hexane containing 100 μL of diphenyl germane) was injected at high pressure from a premixing cell and was flow-through a reaction cell at 1.5–2 mL min^{-1} (denoted as IFT-SFLS growth). In both cases the growth was conducted by the decomposition of diphenyl germane at 375 °C and 20.7 MPa for 60 min in supercritical hexane/CO_2 mixture. After the reaction, the cell was cooled to room temperature, depressurised and the substrate washed with 10 mL of acetone.

Characterization. The surface morphology of the samples was determined by scanning electron microscopy (SEM) on a JEOL, JSM 65007, microscope equipped with an Oxford energy-dispersive X-ray (EDX) detector. The TEM images were obtained with a JEOL 2010 transmission electron microscope operating at 200 kV, equipped with an Oxford EDX detector. Samples for electron microscopy were prepared by the following methods: (i) the alumina matrix was dissolved in phosphoric acid to release the embedded nanowires; (ii) plan-views and cross-sections were prepared by dimple grinding, followed by Ar-ion polishing. The dimple grinding was accomplished using a Gatan dimple grinder Model 656, using 5 μm diamond paste. The precision Ar-ion polishing was done at grazing angles of 6° at 5 kV using a Gatan, precision ion polishing system (PIPS), model 691. XRD measurements were performed on a Philips X'Pert diffractometer using Cu $K\alpha_1$ radiation. The measurements were done in reflection ($\theta-2\theta$) geometry after sample polishing. Electrical properties of the nanostructures embedded within the AAM channels were probed by conductive atomic force microscope (c-AFM) working in contact mode. Samples for c-AFM were prepared as reported previously.[8d] Resistivity values for individual 1D nanostructures within AAMs were calculated using current values obtained from the conductivity maps after measuring the corresponding lengths and cross-sections of the 1D nanostructures by electron microscopy.

(6) (a) Li, G. C.; Papadopolous, J. M.; Xu.; Moskovits, M. *Appl. Phys. Lett.* **1999**, *75*, 367. (b) Guo, Y.-G.; Li, C.-J.; Wan, L.-J.; Chen, D.-M.; Wang, C.-R.; Bai, C.-L.; Wang, Y.-G. *Adv. Funct. Mater* **2003**, *13*, 626. (c) Kovtyukova, N. I.; Kelley, B. K.; Mallouk, T. E. *J. Am. Chem. Soc.* **2004**, *126*, 12738. (d) Wirtz, M.; Martin, C. R. *Adv. Mater.* **2003**, *15*, 455.

(7) (a) Ziegler, K. J.; Ryan, K. M.; Crowley, T. A.; Kulkarni, J.; Polyakov, B.; Erts, D.; Morris, M. A.; Holmes, J. D. *J. Mater. Chem* **2004**, *14*, 585. (b) Cott, D.; Petkov, N.; Morris, M. A.; Platschek, B.; Bein, T.; Holmes, J. D. *J. Am. Chem. Soc.* **2006**, *128*, 3920.

(8) (a) Javey, A.; Nam, S-W.; Friedman, R. S.; Yan, H.; Lieber, C. M. *Nano Lett.* **2007**, *7*, 773. (b) Wang, D.; Tu, R.; Zhang, L.; Dai, H. *Angew. Chem., Int. Ed.* **2005**, *44*, 2925. (c) Xiang, J.; Lu, W.; Hu, Y.; Yan, H.; Lieber, C. M. *Nature* **2006**, *44*, 490. (d) Shan, Y.; Kalkan, A. K.; Peng, C-Y.; Fonash, S. J *Nano Lett.* **2004**, *4*, 2085. (e) Erts, D.; Polyakov, B.; Daly, B.; Morris, M. A.; Ellingboe, S.; Boland, J.; Holmes, J. D. *J. Phys. Chem. B* **2006**, *110*, 820.

(9) (a) Wang, D.; Wang, Q.; Javey, A.; Tu, R.; Dai, H.; Kim, H.; McIntyre, P. C.; Krishnamohan, T.; Saraswat, K. C. *Appl. Phys. Lett.* **2003**, *83*, 2432. (b) Hanrath, T.; Korgel, B. A. *J. Phys. Chem. B* **2005**, *109*, 5518.

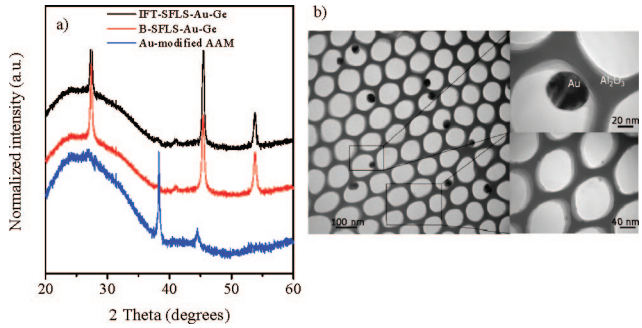

Figure 1. (a) XRD patterns of the amino-modified AAMs impregnated with 0.03 M $AuCl_4$ and reduced for 6 days (blue), and after Ge batch (red) and injection flow-through (black) reactions, and (b) plan-view TEM images of the Au seeds deposited within AAM pores.

Results and Discussion

The assembly of the Au seeds on the walls of the channels running through the AAMs was accomplished by modification of the oxide surface with amine functionalities, followed by wet impregnation of the pores with dilute aqueous $H[AuCl_4]$. Similar approaches have been developed for the deposition of Au nanoparticles in mesoporous silica and anodic alumina surfaces.[10] In the presence of the amine functionality, in situ reduction of the Au^{III} ions takes place in the confined environments at room temperature. This reduction process was followed by UV–visible spectroscopy (see Supporting Information). For example, when discrete Au nanoparticles (5–6 nm in diameter), prepared by the Brust method,[11] were assembled on the surface of the AAMs, absorption originating from excitation of a plasmon resonance was recorded at 520 nm. The absorption spectra form the Au nanoparticles assembled on amine-modified AAMs, and reduced for 6 days or longer, showed broader, slightly red-shifted bands. These results can be explained by the gradual increase in the particle size and deviation from strictly spherical particle shapes.[10] The crystallinity of the Au seeds within the AAMs was confirmed by XRD analysis (Figure 1a). The reflections at 38.1 and 44.2° 2θ can be attributed to metallic Au (JCPDS, reference pattern 01–1172, cubic $Fm\bar{3}m$ structure). The corresponding crystallite sizes determined by applying the Scherer equation to the (111) reflection showed values of about 35 nm. TEM imaging was undertaken to further examine the particle size and shape of the assembled Au nanoparticles on the surface of the amine-modified AAMs (Figure 1b). As observed, after 6 days of reduction well shaped Au nanoparticles were formed having diameters between 25 and 65 nm, in a good agreement with the Au crystallite size determined by the Scherer equation. The nanoparticles were relatively well distributed across the surface of the channels. More careful examination of the membrane surface showed another class of smaller 4–6 nm Au particles, more densely distributed on the alumina surface. All Au nanoparticle populations were firmly bounded to the alumina surface and could serve as seeds in a subsequent SFLS reaction.

The growth of Ge nanostructures within Au-seeded AAMs was observed by cross-sectional SEM, HR-TEM, selected area electron diffraction (SEAD) and EDX measurements. Figure 1a shows XRD patterns of the Au-modified AAMs subjected to batch (B-SFLS-Au-Ge) and injection flow-through (IFT-SFLS-Au-Ge) reactions, respectively. A number of well-resolved reflections at 28.1, 45.5 and 54 degrees 2θ were detected and attributed to crystalline Ge (JCPDS, reference pattern 03–0478, cubic *Fd3m* structure). Applying the Scherer equation to the Ge (111) reflections from the XRD patterns for the B-SFLS-Au-Ge and IFT-SFLS-Au-Ge samples gives a mean diameter for the Ge crystallites of 45 and 120 nm, respectively. For the batch process, the dimensions of the Ge crystallites are similar to those of the Au seeds, and both are smaller than the diameter of the AAMs channels. In contrast, the IFT-SFLS-Au-Ge samples showed average Ge crystalline dimensions larger than the size of the Au seeds and the diameter of the AAMs channels. The Ge nanostructures prepared by the batch reaction showed no preferred orientation with respect to the membrane surface; based on the observation that there was no reduction in the number of reflections or altered intensity ratio of different reflections in the XRD pattern in comparison to the powder Ge reference pattern. Thus randomly oriented Ge crystals, giving rise to powder-like patterns were formed, suggesting a polycrystalline nature of the structures. In comparison, the XRD pattern of the IFT-SFLS-Au-Ge sample showed an altered intensity ratio of the (111) and (220) reflections in comparison to the powder Ge reference patterns. This fact suggests that the {110} family of planes are oriented preferentially and parallel to the membrane surface, thus implying that single crystalline domains are formed having <110> direction as a preferred growth direction. We have previously grown highly oriented and single crystalline semiconductor Bi_2S_3 nanowires within the channels of AAMs using a solventless approach.[12] The XRD analysis of these samples showed remarkable reduction in the number of reflections to a single peak because of the single crystalline and oriented nature of the nanowires.

Further analysis of the crystal structure and the morphology of the Ge nanostructures within the channelled substrates was obtained by electron microscopy. Figure 2a shows a cross-sectional SEM image of the Ge nanostructures grown from a B-SFLS-Au-Ge sample. One dimensional nanostructures can be observed protruding from the channels, and aligned along the direction of the channels. The structures appear grainy, composed of crystalline domains. In comparison, the 1D Ge nanostructures obtained from an IFT-SFLS-Au-Ge sample displayed well-defined nanowire geometries, aligned along the direction of the channels. In both cases, the nanostructures were embedded within the templating matrix while at the same time isolated from each

(10) (a) Petkov, N.; Platschek, B.; Morris, M. A.; Holmes, J. D.; Bein, T. *Chem. Mater.* **2007**, *19*, 1376. (b) Hanaoka, T.; Kormann, H-P.; Kroell, M.; Sawitowski, T.; Schmid, G. *Eur. J. Inorg. Chem.* **1998**, 807. (c) Sehayek, T.; Lahav, M.; Popovitz-Biro, R.; Vaskevich, A.; Rubinstein, I. *Chem. Mater.* **2005**, *17*, 3743.

(11) Brust, M.; Bethell, D.; Kiely, C. J.; Schiffrin, D. J. *Langmuir* **1998**, *14*, 5425.

(12) Xu, J.; Petkov, N.; Wu, X.; Iacopino, D.; Quinn, A. J.; Redmond, G.; Bein, T.; Morris, M. A.; Holmes, J. D. *ChemPhysChem* **2007**, *8*, 235–240.

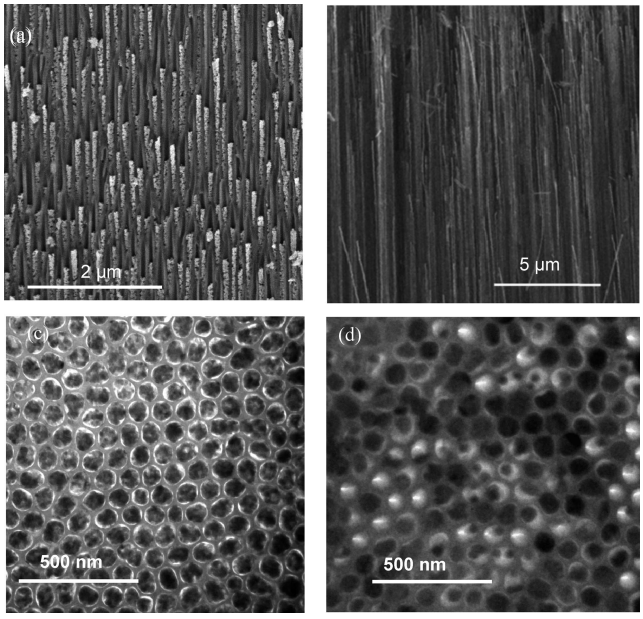

Figure 2. Cross-section SEM images (a) and (b) and plan-view TEM images (c) and (d) of the Ge nanostructures corresponding to the B-SFLS-Au and IFT-SFLS-Au samples, respectively.

other inside the aligned alumina channels. When the nanostructures were imaged in-plan by TEM (images c and d in Figures 2), well-ordered arrays of nanostructures were seen with pore filling factors of approximately 98% and 75% for the B-SFLS-Au-Ge and IFL-SFL-Au-Ge samples, respectively. The corresponding EDX spectra, taken of a large number of nanostructures at several different locations, showed average Al/Ge and Au/Ge atomic ratios of 0.15 and 0.0085 for the B-SFLS-Au-6, and 0.85 and 0.0023 for the IFT-SFLS-Au-12 samples, respectively. The EDX data confirmed a higher loading of Ge and Au within the channels of the B-SFLS-Au-Au-Ge sample and verified that, relatively uniform loadings were achieved across the whole membrane thickness (see the Supporting Information). Oppositely the IFT-SFLS-Au-Ge samples showed nonuniform filling across the membrane surface, with considerable loading factors (reaching those of the B-SFLS-Au-Ge sample) only in the areas close to the membrane outer surfaces, penetrating 15–20 μm deep along the AAMs channels.

Figure 3 shows plan-view TEM images of the deposited nanostructures within the AAMs, imaged with the electron beam parallel to the long axis of the channels. The crystalline nature of the deposited materials within the membrane was examined by dark field imaging and small area electron diffraction (SAED) (usually the SAED patterns were taken on structures deposited within a single channel of the AAMs). The SAED pattern of B-SFLS-Au-Ge samples showed well resolved diffraction rings with *d*-spacings typical for crystalline Ge and Au. The appearance of diffraction rings rather than diffraction spots confirms the polycrystalline nature of the deposited materials. The granular structure of the deposited nanostructures is observed in the dark filed images where the crystalline domain size (brighter objects in the images) can accurately be identified (Figure 3b). The crystalline domain sizes of both Ge and Au are in the range 15–40 nm, in very good agreement with domain sizes determined

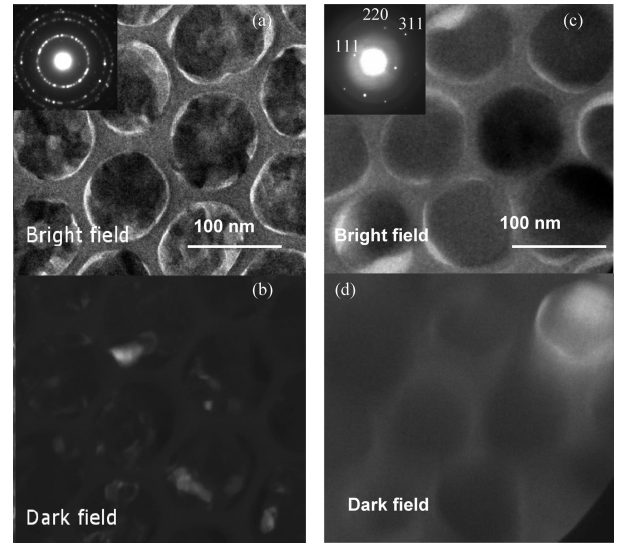

Figure 3. Plan-view (a) bright- and (b) dark-field TEM images of the Ge nanostructures within the B-SFLS-Au, and (c) bright- and (d) dark-field imageswithin IFT-SFLS-Au (insets, corresponding SAED patterns).

form XRD data by the Scherrer equation. In comparison, the dark field image of the nanostructures corresponding to the IFT-SFLS-Au-Ge sample (Figure 3d) highlights one well-shaped nanostructure (brighter object in the image) having dimensions of the channel openings. The SAED pattern of that structure showed well resolved diffraction spots indexed in cubic *Fd3m* symmetry. The indexation of the SAED pattern is done with the electron beam along to the <211> direction, thus exemplifying a case of a Ge nanowire grown along the <211> growth direction. Unique identification of the growth direction of the single crystalline Ge nanowires can be done when a large number of nanostructures are imaged with the electron beam perpendicular to their long axis with simultaneous collection of the SAED and HR-TEM imaging (see below).

To image the 1D nanostructures with the electron beam perpendicular to their long axis the alumina matrix was dissolved in 5% H_3PO_4, or the membranes were prepared as thin cross-sections. TEM images of 1D nanostructures liberated from the B-SFLS-Au-Ge showed well shaped nanowire-like structures, extending for more than several micrometers, and with diameters corresponding to the diameters of the channelled substrates (see the Supporting Information). Most importantly polycrystalline, grainy 1D nanostructures were observed that can be envisioned as Au-nanoparticles (darker spots on the bright filed TEM image) connected through semiconductor Ge crystallites (Figure 4a). In some cases well-defined chains of nanosized Ge-Au segments were observed (see inset in Figure 4a). HR-TEM images further showed crystalline fringes of Ge oriented in all directions, together with Au crystallites (Figure 4c). In contrast, when the IFT-SFLS-Au-Ge sample was imaged as a cross section, well-shaped and encapsulated Ge nanowires were seen (see Supporting Information). One such example is shown in Figure 4b, where a Au nanoparticle can be observed on the tip of the nanowire. The HR-TEM image depicts the single crystalline nature of the nanowire with a lattice spacing of 0.326 nm, corresponding to {111} set of

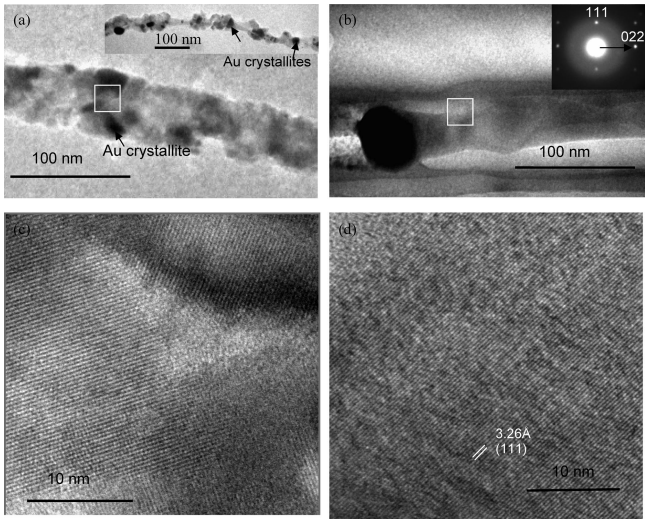

Figure 4. (a) Isolated 1D nanostructures corresponding to the B-SFLS-Au sample (inset, chainlike nanostructures), and (b) cross-sectional TEM image of the IFT-SFLS-Au sample (inset, corresponding SAED pattern), (c, d) corresponding HR-TEM images within marked areas.

planes (Figure 4d). The SAED pattern shown in the inset is of a single crystalline material and is indexed to the *Fd3m* space group with the electron beam along the <211> direction. Thus the nanowire growth direction is determined to be along the <110> direction. This is in a good agreement with the XRD data where the <110> direction was found to be the preferred orientation of the Ge nanostructures within the membranes. Additionally, other growth directions such as <111> and <211> were also observed for the embedded Ge nanowires.

The remarkable difference in the crystallinity of the Ge nanostructures prepared under B-SFLS and IFT-SFLS conditions can be understood in the context of the combined effects played by the SCF media, the Au seeds and the confining environment of the AAMs channels. The B-SFLS reaction is performed at static conditions under supercritical hexane at constant pressure and temperature. These conditions were accomplished by heating the reaction cell (resembling solvothermal methods for growth) until a supercritical state is achieved. Noticeable the difference between this type of growth to other SFLS reactions reported in the literature[3] is that the Au seeds are anchored on the alumina surface and are not organically modified. We suggest that at high temperatures, and in the absence of a stabilizing organic coating layer or a cosolvent (e.g., supercritical CO_2), the Au seeds are highly mobile and reactive. On the other hand the Ge precursors are transported and reacted at a diminished surface tension and at high wettability thus resulting in the efficient conditions for SFLS growth with large numbers of nucleation sites. The growth process can be described as starting from the crystalline facets of the Au seeds and is further guided and restricted by the size and shape of the nanosized channels. We propose that the B-SFLS reaction is ruled by the uniform distribution of the Au seeds, many of them smaller than the AAMs channels, that induce growth of Ge crystallites that are joined together in grainy polycrystalline 1D nanostructures, with high pore filling factors. The growth under IFT-SFLS conditions can be envisioned as a "truly" Au-seeded mecahnism, similar to metal seeded growth of Si or Ge nanowires by CVD,[2] where the diameter of the nanowires and their structure (in this case, single crystalline) is determined predominantly by the dimensions of the Au seeds and the flow-through conditions. Evidence for this mechanism comes from the fact that most of the encapsulated single crystalline nanowires display Au seeds at their tips, whereas some of the Au seeds did not nucleate any growth, resulting in lower filling factors. It appears that injecting the Ge precursors from a supercritical hexane/CO_2 mixture into a cell containing AAMs modified with Au seeds, that were preheated under supercritical CO_2, is a key factor for the deposition of single crystalline Ge nanostructures. The role of the supercritical CO_2 is to work as a cosolvent stabilizing the Au seeds while the flow-through conditions are providing a constant supply of controlled amounts of Ge precursors. The role of the alumina channels is to support the metal seeds and to entrap and align the growing nanowires. Full orientational alignment of the Ge nanowires with respect to the membrane surface was difficult to achieve due to the different growth directions (being primarily along the <110>) with the possible existence of defective nanowires. The latter is probably due to the confining effect of the AAM channels.

The electrical properties of the 1D nanostructures prepared within the channels of the AAMs were probed by c-AFM measurements. Using this approach topography and conductivity maps were obtained simultaneously (Figure 5). It can be seen that points of higher conductivity coincide with the positions of the filled channels, thus providing direct evidence for an ordered array of conductive nanostructures. Resistivity results for B-SFLS-Au-Ge and IFT-SFLS-Au-Ge samples, obtained at room temperature, showed mean resistivites, i.e., resistivity averaged for more than 20 Ge nanostructures, of 0.3 ± 0.2 and 47.7 ± 5.8 ohm m, respectively. The first value lies in the range between bulk resistivities of Ge (0.5 ohm m) and Au (2.2×10^{-8} ohm m), very much closer to the bulk resistivity of Ge. The resistivities measured for the nanostructures within IFT-SFLS-Au-Ge samples were 2 orders of magnitude higher than that of bulk Ge. The noticeable difference in the electrical properties of the two samples lies in the distribution of the resisitivity values (see insets in panels a and b in Figure 6). Although the B-SFLS-Au-Ge sample shows quite a broad range of resistivities (deviating from the mean value by almost 66%), the resistivities for the IFT-SFLS-Au-Ge sample were narrowly distributed, with a standard deviation of approximately 12%. Because the morphology of the 1D nanostructures within the B-SFLS-Au-Ge samples can be described as composed of Au seeds connected through Ge crystallites with a large number of domain boundaries (as seen from XRD and electron microscopy) one would expect that the electrical properties are greatly dependable on the nonuniform nature of the nanostructures, thus very difficult to predict. The resistivity values obtained are within the interval between bulk resistivity of Au and Ge, but very close to the resistivity of bulk Ge, thus suggesting that the material with higher resistivity determines the overall resistivity of the nanostructures. The IFT-SFLS-

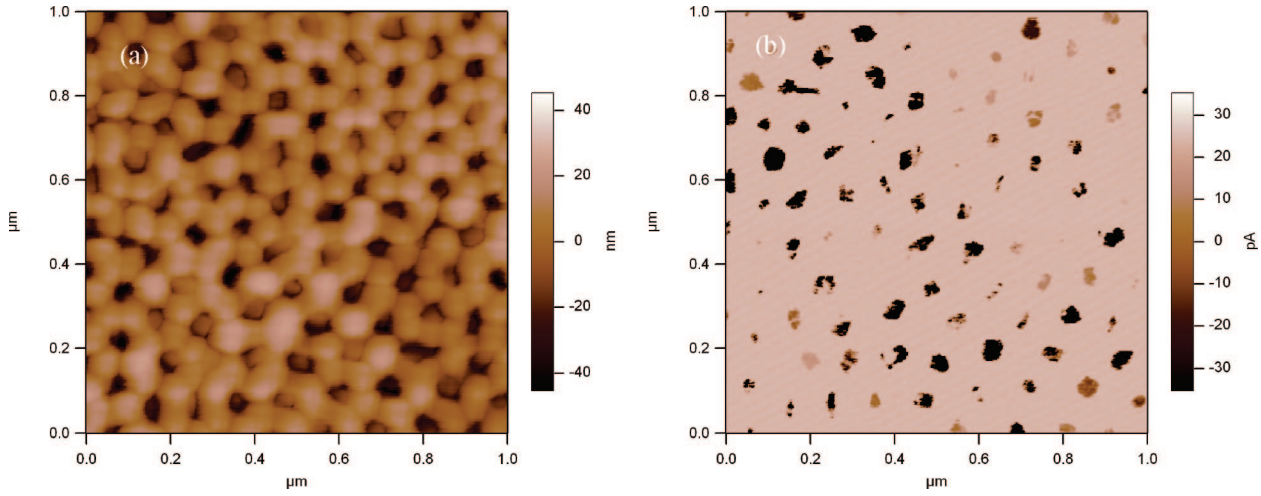

Figure 5. (a) Topography and (b) conductivity maps of representative area from the B-SFLS-Au-6 sample.

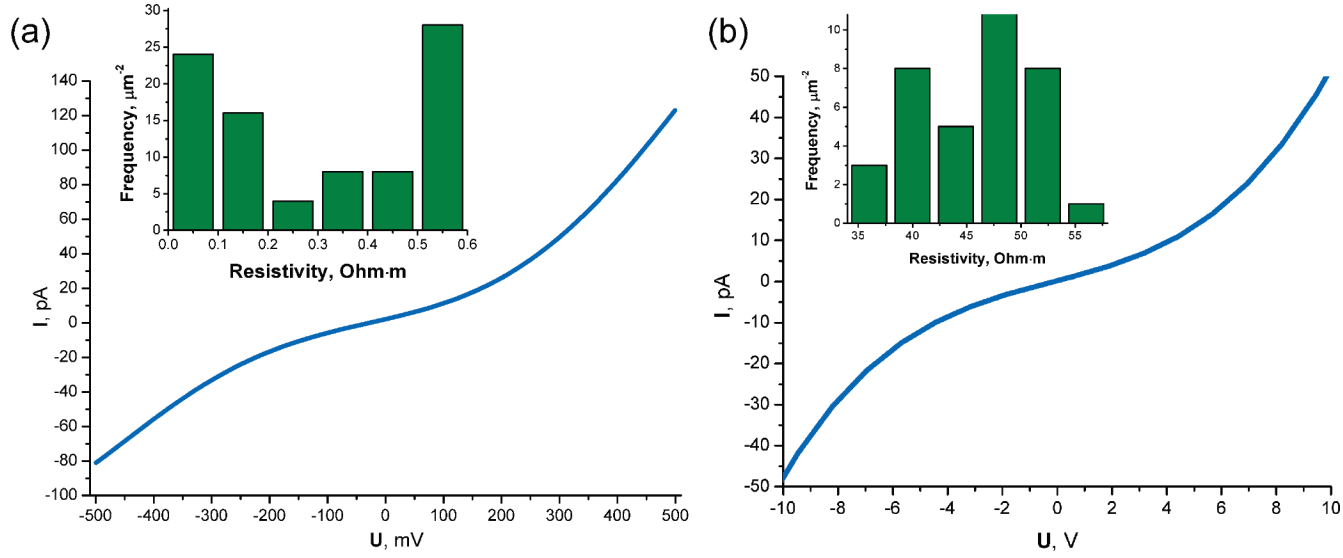

Figure 6. *IV* curves corresponding to individual nanostructures within (a) B-SFLS-Au-6 and (b) IFT-SFLS-Au-12 samples (insets, corresponding distributions of resistivity values calculated from the conductivity maps).

Au-Ge samples have lower amounts of Au seeds positioned at the tips of the nanowires (seen by EDX and microscopy) with relatively uniform and single crystalline morphologies. In this case one would expect resistivity values very close to bulk Ge; though measured resistivities are 2 orders of magnitude higher, their distribution is very sharp, confirming the uniformity of the deposited nanostructures. In both cases, it can be argued that factors such as contact problems and different types of conduction barriers could in some way be influencing the electrical properties of the nanostructure. Additionally, current–voltage (*IV*) characteristics of individual nanostructures corresponding to both samples were measured. Typical *IV* curves, shown in Figure 6(a) and (b), illustrated well-defined nonlinear behavior. This type of behavior may be due to the existence of a Schottky barrier, giving non-uniformity of the tip−nanowire interaction due to the formation of a germanium oxide layer on the surface of the nanowires over short time periods. Nevertheless the 1D nanostructures presented in this work show an improved conductivity of more than 4 orders of magnitude in comparison to similar structures prepared by super-critical inclusion techniques and measured using similar techniques, i.e., 800–3000 ohm m.[8d] Further electrical measurements, including low temperature investigation are currently ongoing, to give further insights into the conduction mechanisms for the Ge nanostructures.

Conclusions

In summary, a new synthetic approach for growing semiconductor nanostructures is presented that relies on the selective modification of channelled alumina surfaces with Au seeds that guide the growth of 1D nanostructures by the SFLS mechanism. Microscopy and XRD measurements reveal that the 1D nanostructures can be obtained with tunable and controllable crystallinity, grain size and domain boundaries, ranging from chains of Au nanoparticles connected through semiconductor Ge crystallites to Au-seeded Ge single-crystalline nanowires. Additionally, the nanostructures are embedded and at the same time isolated from each other inside the channel substrates forming ordered arrays. The Ge growth process can be envisioned as one starting at the crystalline facets of the Au seeds and is further guided and restricted by the size and shape of the nanosized

channels. Conditions that control the type of Ge nanostructures are (i) the distribution and size of the Au seeds across the alumina surfaces, (ii) the type of SCF deposition, e.g., batch vs flow-through deposition and (iii) the confining environment of the AAMs channels. Electrical data showed that resistivities and *IV* curves are considerably improved compared to previous reports for similar systems.

Acknowledgment. The authors thank Science Foundation Ireland (Grant 03/IN3/I375), CRANN (Project PR21), and the Latvian Materials National Program for financial support.

Supporting Information Available: Three additional figures (PDF). This material is available free of charge via the Internet at http://pubs.acs.org.

CM702923K